$$\frac{M}{M_\odot} = 54\, q^{-1}; \qquad L_X = 1.2\times10^{30}\ \mathrm{erg\ s^{-1}}\, q^{-1}\Omega_B^{-1}$$

$$N_0 = 1.3\times10^{9}\ \mathrm{Mpc^{-3}}\, q\Omega_B \tag{5}$$

where $q \equiv \varepsilon_X \Omega_0 \Omega_B T_{04}^{-3/2} \mu_0^{-3}$ is expected to be $\ll 1$. Hence such objects must be supermassive black holes. These constraints can be generalized to a power law mass spectrum of compact objects, say $dN/dM \propto M^{-\gamma}$ for $M_1 \leq M \leq M_2$. Then the mass constraint in equation (5) applies approximately to M_2 for $\gamma < 2$ or M_1 for $\gamma > 3$.

The strongest constraint on the parameters in equation (5) comes from the sources count and fluctuation limit. From Uhuru and Ariel 5 small scale fluctuations ($\delta I/I \leq 2.5\%$ at 0.004 sr beam width), Schwartz[9] already puts an upper limit on possible contribution of unknown classes of discrete sources to K (number of sources with $S > 1$ UFU per sr) < 10. The Einstein survey gives $K \simeq 7 \pm 3$ for all sources[3], most of which have optical images. In the preliminary Draco and Eridanus surveys, only three out of 43 sources have empty optical fields[3]. Hence it seems reasonable to put a conservative upper limit for the contribution of accreting intergalactic black holes to the source count

$$K_B \leq 2 \tag{6}$$

Future observations may further lower this limit. As most such contributions would come from $Z \leq 1$ we have (see ref. 9):

$$K_B \simeq 3.7\times10^{6} L_{X44}^{3/2} N_0;\ L_{X44} = L_X/10^{44}\ \mathrm{erg\ s^{-1}} \tag{7}$$

Combining equations (5), (6) and (7) we have:

$$\varepsilon_X^{1/2}\Omega_B \geq 3.2\times10^{-6}\Omega_0^{-1/2} T_{04}^{3/4}\mu_0^{3/2} \tag{8}$$

$$L_X \leq 1.2\times10^{41}\ \mathrm{erg\ s^{-1}} \tag{9}$$

$$M/M_\odot \leq 1.7\times10^{7}\, \varepsilon_X^{-1/2}\Omega_0^{-1/2} T_{04}^{3/4}\mu_0^{3/2} \tag{10}$$

$$N_0 \geq 1.3\times10^{-2}\ (\mathrm{Mpc})^{-3} \tag{11}$$

For the IGG proposed by Sargent *et al.*[6] with $\Omega_0 \sim 0.1$, $T_{04} \sim 1$ and $\mu_0 \sim 10$ we find $\Omega_B \geq 3\times10^{-4}\,\varepsilon_X^{-1/2}$ and $M \leq 2\times10^{9} M_\odot \varepsilon_X^{-1/2}$.

If the IGG contains even a minute amount of organized angular momentum, the accretion flow will turn into a disk near the black hole[10] where most of the X-ray is emitted, in which case ε_X could be high. The familiar disk model with optically thin TB emission has maximum temperature $T_e \sim 10(M M_\odot/M)^{1/2}$ provided $10^7\ K \ll T_e \leq 10^9$ K (ref. 11). If we set this to the observed CXB TB temperature we find (see equation (5))

$$\varepsilon_X \Omega_B \sim 10^{-7} \tag{12}$$

When equation (12) is combined with equations (8) and (5) we get the constraints

$$\varepsilon_X \leq 10^{-3}\,\Omega_0 T_{04}^{-3/2}\mu_0^{-3};\ \Omega_B \geq 10^{-4}\,\Omega_0^{-1} T_{04}^{3/2}\mu_0^{3}$$

$$\frac{M}{M_\odot} \sim 5\times10^{8}\,\Omega_0^{-1} T_{04}^{3/2}\mu_0^{3} \tag{13}$$

These numbers are uncertain to the extent the TB disk models are. Also, the requirement that the IGG is not depleted by accretion in a Hubble time demands $\varepsilon_X \Omega_B \geq 10^{-8}$. The above results are summarized in Fig. 1.

We conclude that it is possible that much of the CXB is produced by the hot TB emission of Sargent type IGG accreting onto intergalactic black holes in the present epoch ($Z \leq 3$). This picture then predicts the existence of a new class of faint ($L_X \leq 10^{41}$ erg s^{-1}), numerous ($N_0 \geq 10^{-2}$ Mpc^{-3}) and low mass ($M \sim 10^7$–$10^{10} M_\odot$) discrete sources without optical or IR images. Gorenstein has pointed out that such objects may be separated from (optically) faint QSOs in the Einstein survey by studying the distribution of the lower limits to their $L_X/L_{optical}$ ratio (P. Gorenstein, personal communication). Note that the bulk of such sources are fainter than the limit of the HR I of Einstein so their predicted $N \propto S^{-1.5}$ does not conflict with the observed steeper distribution. Note that these masses overlap with the mass corresponding to nonlinear density clumps

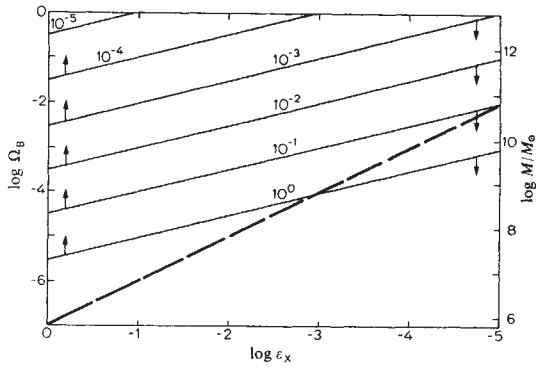

Fig. 1 Solid curves give the lower limit on Ω_B and upper limit on M as provided by the source count limit $K_B \leq 2$. The number on each curve labels the value of $\omega \equiv \Omega_0^{1/2} T_{04}^{-3/4} \mu_0^{-3/2}$ of the IGG (see equation (5)). The dashed curve represents the constraint on Ω_B for the TB disk model to give the observed CXB temperature. In this case M is independent of Ω_B or ε_X (see equation (13)).

($\delta\rho/\rho \sim 1$) at decoupling as extrapolated from the present power law density correlation function[12,13]. Some of such clumps could (but need not) directly collapse into black holes without fragmenting into stellar systems at $Z \geq 10$ and their X-rays could have Compton-heated the denser IGG[7]. In such case the IGG would not evolve adiabatically and Carr finds that the direct contribution of accretion to the CXB at $Z = 10$ may also be significant[7].

I thank B. J. Carr for his pregalactic black hole results before publication, also D. Sciama, V. Petrosian and P. Gorenstein for helpful discussions.

Received 11 December 1979; accepted 24 April 1980.

1. Boldt, E. A. Preprint NASA TM-78106 (1978).
2. Field, G. B. & Perrenod, S. C. *Astrophys. J.* **215,** 717 (1977).
3. Giacconi, R. *et al. Astrophys. J. Lett.* (in the press).
4. Tananbaum, H. *et al. Astrophys. J. Lett.* (submitted).
5. Setti, G. & Woltjer, L. *Astr. Astrophys.* **76,** LI (1979).
6. Sargent, W. *et al. Astrophys. J.* (submitted).
7. Carr. B. J. *Mon. Not. R. astr. Soc.* **189,** 123 (1979).
8. Bondi, H. *Mon. Not. R. astr. Soc.* **112,** 195 (1952).
9. Schwarz, D. in *X-Ray Astronomy* (ed. Baity, W. A. & Peterson, L. E.) (Pergamon, Oxford, 1979).
10. Pringle, J., Rees, M. J. & Pacholczyk, A. G. *Astr. Astrophys.* **29,** 179 (1973).
11. Eardley, D. M., Lightman, A. P., Payne, D. G. & Shapiro, S. L. *Astrophys. J.* **224,** 53 (1978).
12. Gott, J. R. III & Rees, M. J. *Astr. Astrophys.* **45,** 415 (1975).
13. Peebles, P. J. E. *Astrophys. J. Lett.* **189,** 251 (1974).

Discontinuities in the jovian plasma disk of sulphur and oxygen ions

W.-H. Ip

Max-Planck-Institut für Aeronomie, D-3411 Katlenburg-Lindau 3, FRG

The process of local acceleration of the plasma cloud freshly ejected from Io into the jovian magnetosphere is considered here. A physical model previously employed to investigate the motion of artificial barium cloud, is used to estimate the time scale for such transient acceleration. In normal conditions, the new ions could be accelerated to full corotation within $\sim 3\times 10^2$s of injection. But the corresponding time scale might be increased 10-fold or so at the peaks of mass injection. In this way the observations of non-rigid corotation of the S ions of sporadic nature may be understood. The temperature and ionization discontinuities in the Io torus as observed by the Voyager experiments is also considered. Here we propose that such a sharp transition is related to the coupling of the radial diffusion and heating plus cooling of the thermal plasma.

0028-0836/80/270040-04$01.00

Ground-based observations[1-6] indicate that the S optical emissions of the jovian sulphur nebula at 6,717 and 6,730 A usually have a very sharp cutoff at, or inside of, the orbit of Io at 6 R_J, whereas the inner boundary between 3 and 4 R_J has a diffuse appearance. At the same time, it has been established that the motion of the sulphur ions in this nebula is in corotation with the jovian magnetosphere[1]. Although these descriptions may be considered to represent the norm of the S^+ plasma disk, Mekler *et al.*[7] have recently presented evidence of occasional weak S^+ emission outside the orbit of Io. Particularly interesting are the velocities of the S^+ ions in this anomalous emission. Although the motion of the S^+ plasma inside of the sharp boundary was in rigid corotation, the corresponding motion in the outer emission was slower than would be expected for corotation. Such unusual phenomena may be caused by some disturbances in the jovian magnetosphere (for example, substorms), or simply related to the injection process of the sulphur ions from Io. [Note that evidence of non-rigid corotation (up to a few per cent) of the jovian magnetospheric plasma in the vicinity of the orbit of Io have been recently reported[8,9] on the basis of plasma wave and planetary radio astronomy experiments. These observations are presumably more representative of the quiescent state of the Io torus.]

A model formulated by Scholer[10] to study the motion of ionized barium cloud artificially released in the Earth's magnetosphere[11,12] will now be applied to the case of the Io torus of sulphur and oxygen ions. Although highly simplified, this treatment gives a reasonable approximation to the MHD transfer of angular momentum from Jupiter to the Io torus and the resultant heating of the ion cloud. This model together with considerations on the radial diffusion and cooling of the ion cloud, and the new information from the Voyager 1 and 2 observations of the jovian system[13-18], would allow us to interpret systematically the non-corotation events and several other related observations.

The geometry of the MHD coupling between the Io torus and the jovian ionosphere will first be represented by a two-dimensional system with both the ionosphere and the ion cloud idealized as flat slabs of finite vertical thickness and width in the y-direction, and the extension in the x-direction is supposed to be infinite, see Fig. 1. The planetary magnetic fields of uniform strength B are pointing in the z-direction. Furthermore, the magnetosphere between the ionosphere and the Io torus is assumed to have a plasma density of ρ, while the surface density of the torus is m_0 (in g cm^{-2}). The motion of the torus is then coupled to that of the ionosphere through the continuous transmissions and reflections of the Alfvén waves propagating between these two regions[19] with acceleration of the ion cloud as the end result.

More specifically, as the waves travel through the magnetosphere with the Alfvén speed $V_A = B/(4\pi\rho)^{1/2}$ there will be a polarization current j_p carried at the wave fronts[10,20-23]. As shown in Fig. 1*a*, the current will be closed in such a way that the $\mathbf{j}\times\mathbf{B}$ forces would decelerate the magnetospheric, or the ionospheric, plasma but accelerate the ion cloud. The total polarization current can be expressed as $I_p = \sum_A \mathbf{E}\uparrow$, where $\mathbf{E}\uparrow$ is the electric field applied at the (upward going) wave front and $\sum_A = c^2/4\pi V_A$ is the so-called wave conductivity of the magnetosphere. As the wave reaches the ionosphere with a height-integrated Pedersen conductivity $\sum$, an electric field $\mathbf{E}\downarrow$ will be reflected, whereas a conduction current $I_\perp = \sum(\mathbf{E}\uparrow - \mathbf{E}\downarrow)$ will be set up flowing across the magnetic field.

As the ionospheric conduction current must be equal to the total current in the magnetosphere, that is:

$$\sum(\mathbf{E}\uparrow - \mathbf{E}\downarrow) = \sum_A(\mathbf{E}\uparrow + \mathbf{E}\downarrow) \tag{1}$$

we have the following relationship between the incoming and reflected waves:

$$\mathbf{E}\downarrow = \left[\frac{1-X}{1+X}\right]\boldsymbol{E}\uparrow \tag{2}$$

with $X = \sum/\sum_A$. Thus, the reflection coefficient of the Alfven waves at the ionospheric boundary is given by $\alpha = (1-X)/(1+X)$. From the same reasoning we can see that after a time $T_A = 2L/V_A$, which is the characteristic time for an Alfven wave to travel back and forth between the ion cloud and the ionosphere, there will be another reflection, and so on. The acceleration of the ion cloud is, therefore, not just a function of the ratio between $\sum$ and $\sum_A$ but also time t. Another important factor in this dynamical problem is the distributed mass of the ion cloud. Assuming that the central slab is initially at rest (which is pertinent to the case when an ion cloud is just ejected from Io) and taking the inertia of the ion cloud into account, a general solution for the velocity of the cloud can be derived as was done by Scholer[10] for the barium cloud release experiments. In the present context we have

$$V(t) = V_0\{1 - \sum_{n=0}(-1)^n\alpha^n[\exp(-t_n/T_0)L_n(2t_n/T_0) + \alpha\exp(-t_{n+1}/T_0)L_n(2t_{n+1}/T_0)]\} \tag{3}$$

Here $t_n = t - nT_A$, $T_0 = 2m_0V_A/B^2$, V_0 is the corotation speed, and the summation is carried out only for the Laguerre polynomials $L_n(t_n)$ with $t_n \geq 0$. The normalized velocity profiles for various combinations of T_0, T_A, and α are shown in Fig. 2.

Briefly, for $\sum \gg \sum_A$ and hence $\alpha \approx -1$, the MHD coupling between the ionosphere and the ion cloud is very strong, and in the case of small T_A/T_0 ratio the ion cloud will be accelerated to full corotation speed in just a few times of T_A. On the other hand, if $\sum \ll \sum_A$ and hence $\alpha \approx 1$, the motion of the ion cloud is only weakly coupled to the ionosphere by Alfvén waves. Acceleration of the ion cloud would be very slow. The inertia effect of the ion cloud can also be observed by examining the velocity profiles with different T_A/T_0 ratios but the same value of α.

To explore this result further we assume, for example, the magnetospheric plasma density to be ≈ 1 proton cm^{-2}, the surface number density n_s of the ion cloud just ejected from Io to be $\approx 2\times10^{12}$ ions cm^{-2}, and the length scale L to be $\approx 10R_J$; the

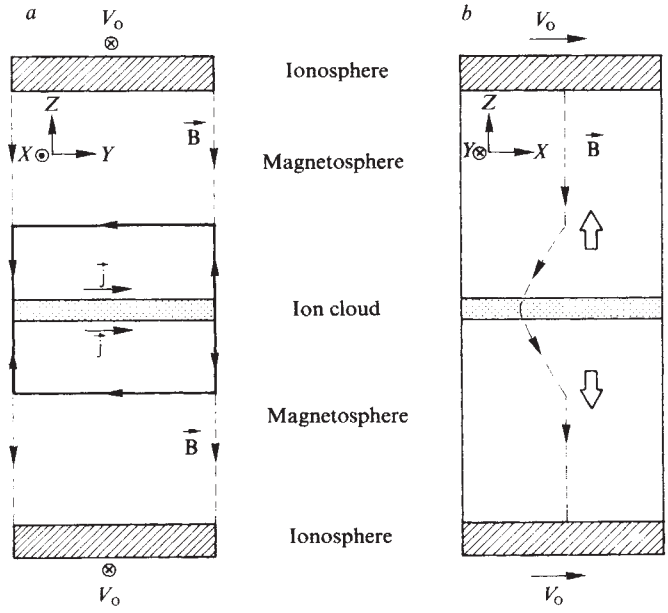

Fig. 1 *a*, A cross-section of the model in the Y–Z plane. The wave current system decelerating the magnetosphere and accelerating the ion cloud is sketched. As a result of the successive transmissions and reflections of these guided waves, a field-aligned current system will be established between the ionosphere and the Io cloud, similar to the current system detected in the vicinity of Io[21,40-43]. The auroral hiss observed on the inner edge of the torus at $L \approx 5.6$ R_J (ref. 43) is probably caused by the beaming of low energy electrons (10 eV–1 keV) associated with such current flows. *b*, A finite section of the model in the X–Z plane. The upward and downward propagations of the Alfvén waves are indicated.

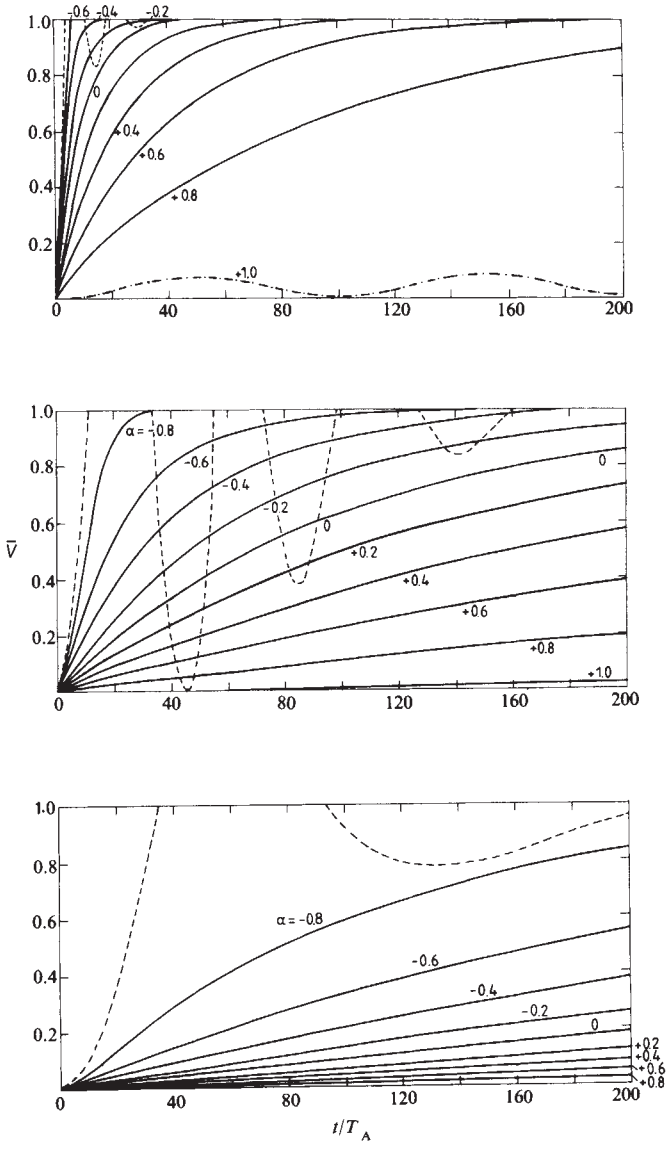

Fig. 2 Velocity profiles of the ion cloud (initially at rest) normalized to the corotation velocity V_0 for various values of the T_A/T_0 ratio and the reflection coefficients α. For $\alpha \leqslant -0.6$, $\sum \geqslant 4\sum_A$. If the plasma density in the magnetosphere is 1 proton cm^{-3}, and $B = 2\times10^3$ nT we have $\sum_A \geqslant 0.02$ S, consequently $\sum \geqslant 0.1$ S. In this MHD approximation, the ion cloud velocity oscillates before reaching the corotation velocity for $\alpha \to -1$ (see dashed lines). A more realistic description is for the ion cloud to be accelerated to the full speed without such overshoots. *a*, $T_A/T_0 = 10^{-1}$; *b*, $T_A/T_0 = 10^{-2}$; *c*, $T_A/T_0 = 10^{-3}$.

value of the ratio T_A/T_0 can then be approximated to be ≈ 0.1. (As the total ejection rate can be written as $\dot{N} \approx 2n_0 R_s V_0$, $\dot{N} \approx 5\times10^{27}$ ions s^{-1} if $n_s \approx 2\times10^{12}$ and R_s is the radius of Io. This value is compatible with the production rate of the sulphur and oxygen ions as estimated by Broadfoot *et al.*[15].) As the S^+ nebula was generally observed to be in rigid corotation with the jovian magnetosphere, the characteristic time scale for the corresponding acceleration of the ion cloud probably is no more than a few times of T_A. Thus the α value may be taken to be $\leqslant -0.6$, or $\sum/\sum_A \geqslant 4$, say. With $T_A \approx 30$ s and $V_0 = 57$ km s^{-1}, Fig. 2 shows that the ions picked up directly from the ionosphere/exosphere of Io will be accelerated to full corotation within 10 Io radii. This trail of slow moving ions may be interpreted as the wake of the satellite ionosphere[24–26]. (This picture would still hold qualitatively for the interaction of Io with the torus of dense hot plasma.)

Now, if the ejection rate N were occasionally increased by a factor of 10 or so (for example, at the maximum of volcanic activities if ionospheric loss is the dominant injection process), $T_A/T_0 \leqslant 0.01$ and the resulting acceleration time scale will be lengthened by a similar factor. Thus, after its first ejection from Io, the ion cloud would probably stay behind corotation for at least an hour, leaving an ion wake ~150° long. This non-corotation effect could persist even longer if the volcanic activity lasts more than a few hours. The large mass of the fresh S and O^+ ions injected in these events, of course, would enable the non-rigid corotation behaviour to be discerned more easily, especially outside the nominal edge of the S II nebula.

If the non-corotation of the weak emission of S^+ ions observed outside the nominal outer edge[7] could be explained by the inertia effect of the MHD acceleration process plus the sporadic outbursts of the volcanic activities, how do we explain the simultaneous corotation of the S^+ ions observed in the inner region of stronger emission? And above all, why should there be a sharp discontinuity confining the S^+ emission within 6 R_J in the first place. These questions may be answered by referring to the Voyager observations of the Io torus. First, the EUV experiment[15] and the plasma experiments[16] have found that the bulk of the heavy ions is apparently in the form of S^2 , S^3 , and O^{2+} with thermal temperature $kT \approx 5$–50 eV. This hot ion torus—with its point of maximum number density approximately located at 5.8 R_J—has $5R_J$ as its inner boundary and 7–8 R_J the outer boundary. Second, a sharp drop in temperature from $kT \approx 10$ eV to 1 eV was found at 5.7 R_J by the plasma experiments[16]. Together with the temperature change, there is also an apparent change in the ionization state of the heavy ions from S^{2+}, O^{2+} to S^+ and O^+. Such stratification of the plasma temperature and ionization might be related to the balance between ionization equilibrium and thermal equilibrium as was found in the structures of planetary nebulae[27–29]. Note that the ions freshly created in the vicinity of Io can have kT as high as 260 eV for O^+ and 520 eV for S^+ (ref. 30) the maximum time scale for cooling of these new ions[31] can be calculated to be $t_c \leqslant 1.5\times10^5$s. In comparison, adopting a radial diffusion coefficient of 10^{-6} R_J^2 s^{-1} (ref. 32), the time scale for diffusion across a distance of 0.5 R_J at this region is $t_d \approx 7\times10^4$s. As $t_d \geqslant t_c$, the heating of the Io torus is then limited to a distance of less than 0.5 R_J around the orbit of Io. Although this may partly explain the sharp division between the hot and cold plasma at 5.7 R_J, issue could be raised about the absence of such discontinuity at 6.3 R_J or so. An explanation of such asymmetric behaviour may come from the additional heating effect beyond 6 R_J as a result of Landau damping of the ion cyclotron waves, for example (ref. 33 and C. K. Goertz, personal communication). We may argue that the energetic (S^+ and O^+) ions, which are responsible for generation of the ion cyclotron turbulence, would not be able to diffuse across Io due to its absorption effect; and this in turn would limit the plasma wave activities and hence plasma heating to radial distance >5.9 R_J.

The ionization state and thermal condition of the Io plasma disk is therefore determined by four inter-related time-dependent processes, namely: (1) the ejection rate; (2) the MHD acceleration; (3) the radial diffusion; and (4) the cooling and heating of the ion cloud. Not just the structure of the 'quiescent' S^+ nebula and the non-corotation of the anomalous emission during the 'disturbed' periods, but also the temperature and density discontinuities together with the apparent ionization stratification in the Io torus can be explained in this way.

While we have concentrated on the local and transient effect acceleration of the plasma just ejected from Io, clearly the time-averaged acceleration and transfer of angular momentum of the Io torus in a more global scale must be of the same vein. For a description of the non-rigid corotation of the jovian magnetospheric plasma at radial distances beyond $6R_J$ see refs 34–36. Alternative views on the asymmetric radial distribution of the thermal plasma[37,38] addressing the possibility of two different diffusion mechanisms at both sides of Io had also been proposed. The effect of such process on our hypothesis of the temperature and ionization discontinuity remains to be investi-

gated. The recent report by Shemanski that an upper limit of 10^{27} ions s^{-1} may be derived for the ion source in the vicinity of Io is also problematic as it sets a stringent condition on the model of local mass pick up[25,26]. In any event, our primary result for the transient acceleration of the Io plasma cloud is by no means affected because, in principle, it is valid for both local (ionospheric scavenging) and more extended (ionization of the sputtered atoms) ion sources.

I thank Dr C. K. Goertz for useful discussions on the problem of magnetospheric propagation of the Alfvén waves.

Received 5 February; accepted 30 April 1980.

1. Kupo, I., Mekler, Yu. & Eviatar, A. *Astrophys. J. Lett.* **205,** L51 (1976).
2. Brown, R. A. *Astrophys. J. Lett.* **206,** L179 (1976).
3. Brown, R. A. *Astrophys. J. Lett.***224,** L97 (1978).
4. Mekler, Yu., Eviatar, A. & Kupo, I. *J. geophys. Res.* **82,** 2809 (1977).
5. Munch, H., Trauger, J. T. & Roesler, F. L. *Bull. Am. astr. Soc.* **9,** 465 (1977).
6. Pilcher, C. B. *Bull. Am. astr. Soc.* **10,** 579 (1978).
7. Mekler, Yu., Eviatar, A. & Siscoe, G. L. *Mon. Not. R. astr. Soc.* **189,** 15 (1979).
8. Kurth, W. S., Gurnett, D. A. & Scarf, F. L. *Geophys. Res. Lett.* **7,** 61 (1980).
9. Kaiser, M. L. & Desch, M. D. *NASA Tech. Mem.* 80626 (Goddard Space Flight Center, 1980).
10. Scholer, M. *Planet. Space Sci.* **18,** 977 (1970).
11. Biermann, L., Lüst, R., Lüst, Rh. & Schmidt, H. U. *Z. Astrophys.* **53,** 226 (1961).
12. Haerendel, G., Lüst, R. & Rieger, E. *Planet. Space Sci.* **15,** 1 (1967).
13. Smith, B. A. *et al. Science* **204,** 951 (1979).
14. Smith, B. A. *et al. Science* **206,** 927 (1979).
15. Broadfoot, A. L. *et al. Science* **204,** 979 (1979).
16. Bridge, H. S. *et al. Science* **204,** 987 (1979).
17. Scarf, F. L., Gurnett, D. A. & Kurth, W. S. *Science* **204,** 991 (1979).
18. *Nature* **280,** 725–806 (1979).
19. Kendall, P. C. *Astrophys. J.* **129,** 194 (1959).
20. Drell, S. D., Foley, H. M. & Ruderman, M. A. *J. geophys. Res.* **70,** 3131 (1965).
21. Neubauer, F. M. *J. geophys. Res.* **85,** 1171 (1980).
22. Maltsev, Yu. P., Leontyev, S. V. & Lyatsky, W. B. *Planet. Space Sci.* **22,** 1519 (1974).
23. Maltsev, Yu.P., Lyatsky, W. B. & Lyatskaya, A. M. *Planet. Space Sci.* **25,** 53 (1977).
24. Cloutier, P. A., Daniell, R. E. Jr, Dessler, A. J. & Hill, T. W. *Astrophys. Space Sci.* **55,** 93 (1978).
25. Ip, W.-H. & Axford, W. I. *Nature* **283,** 180 (1980).
26. Goertz, C. K. *J. geophys. Res.* (in the press).
27. Harrington, J. P. *Astrophys. J.* **152,** 943 (1968).
28. Harrington, J. P. *Astrophys. J.* **156,** 903 (1969).
29. Miller, J. S. *A. Rev. Astr. Astrophys.* **12,** 331 (1974).
30. Siscoe, G. L. & Chen, C. K. *Icarus* **31,** 1 (1978).
31. Spitzer, L. Jr *Physics of Fully Ionized Gases* 2nd edn, 135 (Interscience, New York, 1962).
32. Mogro-Campero, A. in *Jupiter* (ed. Gehrels, T.) 1190 (University of Arizona Press, 1976).
33. Eviatar, A., Mekler, Y. & Coroniti, F. V. *Astrophys. J.* **205,** 622 (1976).
34. Hill, T. W. *J. geophys. Res.* **84,** 6554 (1979).
35. Hill, T. W. *Science* **207,** 301 (1980).
36. McNutt, R. L. Jr, Belcher, J. W. Sullivan, J. D., Bagenal, F. & Bridge, H. S. *Nature* **280,** 803 (1979).
37. Froideraux, L. *Geophys. Res. Lett.* **7,** 33 (1980).
38. Richardson, J. D., Siscoe, G. L., Bagenal, F. & Sullivan, J. D. *Geophys. Res. Lett.* **7,** 37 (1980).
39. Shemanski, D. *3rd Conf. on the Jovian Magnetosphere,* Houston (1980).
40. Ness, N. F. *et al. Science* **204,** 982 (1979).
41. Piddington, J. H. & Drake, J. F. *Nature* **217,** 935 (1968).
42. Goldreich, P. & Lyndell Bell, D. *Astrophys. J.* **156,** 59 (1969).
43. Gurnett, D. A., Kurth, W. S. & Scarf, F. L. *Nature* **280,** 767 (1979).

S-wave anisotropy in the upper mantle under a volcanic area in Japan

Masataka Ando & Yuzo Ishikawa*

Disaster Prevention Research Institute, Kyoto University, Uji, Kyoto 611, Japan

Hiroo Wada

Kamitakara Crustal Movement Observatory, Disaster Prevention Research Institute, Kyoto University, Kamitakara, Gifu 506-13, Japan

Most ultra-basic nodules that probably originated in the upper mantle have anisotropic petrofabric and elastic properties[1,2]. Within seismology, however, the Earth is generally assumed to be isotropic and this assumption is appropriate for most seismological studies. Thus, rocks can be considered isotropic on large scales although anisotropic on a scale of hand specimen[3]. This interpretation is questionable, however, in light of the increasing resolution of seismic observations. Many reliable reports on seismic anisotropies have been accumulating: for example, azimuthal anisotropy in P_n velocities in oceanic basins[4], and in the continent[5] and the back-arc basin[6], and an S-wave splitting of the SH and SV waves revealing an anisotropic structure as deep as 190 km (ref. 7). These suggest that some unsuccessful detections of the Earth's anisotropies may be due to lack of appropriate observations. We describe here the recent discovery of shear wave anisotropy in a volcanic area in Japan, which was revealed by an improvement in the seismographic observation systems.

Telemetery systems of the seismographic stations have recently been established by Kyoto and Nagoya Universities[8] (Fig. 1) in the Chubu area, Japan, beneath which the Pacific plate is subducting. This instrumental development improves the spatial coverage, timing accuracy and recording conditions of seismic observations. The Kamitakara Observatory of Kyoto University is located in the northern part of this area[9] (Fig. 1). Immediately beneath the observatory (Takayama area), at a depth of ~260 km (ref. 10) there are often deep earthquakes. These are very useful events for studies of structures within the wedge between the subducting plate and the Earth's surface in the island arc. As seismic ray paths from these events to the seismographic stations are almost vertical, the wave forms are quite simple because of little contamination of converted waves generated at conspicuous layer boundaries. The stations AMJ and KTJ of this observatory are equipped with the three-component seismographs and the station NRJ with a vertical component one only. The natural pendulum period T_0 is 1 s for both vertical and horizontal seismographs.

Figure 2*a* shows seismograms of one of those deep earthquakes (the earthquake 1 in Fig. 1 and Table 1) recorded at the Kamitakara Observatory. Because the P-wave arrives at the three stations within 0.2 s, the incidence angle is less than 5°. Remarkably, the horizontal seismograms show two distinct arrivals of the shear wave, a fast arrival for the NS component and a slower arrival for the EW one. The horizontal seismograms of three more earthquakes from the same area (earthquakes 2, 3 and 6 in Fig. 1 and Table 1) were examined. These seismograms showed the two different arrivals of the S-wave similar to that in Fig. 2*a*. Such differences in the arrival time of the S-wave between the two horizontal components would be caused by interference of converted waves, but for the present case this interpretation should be dismissed. No significant signal is in fact observed on the vertical component in Fig. 2*a*. A probable interpretation is that S-wave splitting is caused by anisotropy of the medium at intermediate locations between earthquake source and seismographic stations. The incident S-wave is generally resolved into two shear waves that travel along the same path with different velocities—a phenomenon known as acoustic 'double refraction'[11].

As the directions of horizontal seismographs, NS and EW, are not necessarily those of the principal axes of anisotropy, the two split shear waves are generally not resolved on the two horizontal seismograms. Figure 2*a* implies, however, that the directions of the principal axes of the anisotropy are rather close to NS and EW. To determine precise directions of the velocity axes, we synthesized the S-wave forms, by rotating the two orthogonal axes in a clockwise direction at an interval 15°, and projecting the observed S-wave particle motion onto the rotated axes. When a rotation angle θ from the north or east coincided with a principal axis, the two orthogonal S-waves became most widely separated. As shown in Fig. 2*b*, $\theta = 15°$ seems to provide the clearest separation for both records of AMJ and KTJ. The azimuth of maximum velocity, thus, is N15°E and the azimuth of minimum velocity is E15°S.

Present address: Geophysical Research Institute, State Seismological Bureau, Peking, People's Republic of China.

0028-0836/80/270043-04$01.00